Received: 15 January 2020 | Revised: 7 April 2020 | Accepted: 9 April 2020

DOI: 10.1002/jcc.26213

FULL PAPER

Journal of COMPUTATIONAL CHEMISTRY WILEY

How accurate are TD-DFT excited-state geometries compared to DFT ground-state geometries?

Jun Wang[1,2] | Bo Durbeej[1]

[1]Division of Theoretical Chemistry, IFM, Linköping University, Linköping, Sweden

[2]Institut de Química Computacional i Catàlisi, Facultat de Ciències, Universitat de Girona, Girona, Spain

Correspondence
Bo Durbeej, Division of Theoretical Chemistry, IFM, Linköping University, SE-58183, Linköping, Sweden.
Email: bodur@ifm.liu.se

Funding information
Linköpings Universitet, Grant/Award Number: N/A; Stiftelsen Olle Engkvist Byggmästare, Grant/Award Number: 184-568; Vetenskapsrådet, Grant/Award Number: 2019-03664

Abstract

In this work, we take a different angle to the benchmarking of time-dependent density functional theory (TD-DFT) for the calculation of excited-state geometries by extensively assessing how accurate such geometries are compared to ground-state geometries calculated with ordinary DFT. To this end, we consider 20 medium-sized aromatic organic compounds whose lowest singlet excited states are ideally suited for TD-DFT modeling and are very well described by the approximate coupled-cluster singles and doubles (CC2) method, and then use this method and six different density functionals (BP86, B3LYP, PBE0, M06-2X, CAM-B3LYP, and ωB97XD) to optimize the corresponding ground- and excited-state geometries. The results show that although each hybrid functional reproduces the CC2 excited-state bond lengths very satisfactorily, achieving an overall root mean square error of 0.011 Å for all 336 bonds in the 20 molecules, these errors are distinctly larger than those of only 0.004–0.006 Å with which the hybrid functionals reproduce the CC2 ground-state bond lengths. Furthermore, for each functional employed, the variation in the error relative to CC2 between different molecules is found to be much larger (by at least a factor of 3) for the excited-state geometries than for the ground-state geometries, despite the fact that the molecules/states under investigation have rather uniform chemical and spectroscopic character. Overall, the study finds that even in favorable circumstances, TD-DFT excited-state geometries appear intrinsically and comparatively less accurate than DFT ground-state ones.

KEYWORDS

ab initio methods, aromatic organic compounds, benchmark, density functional theory, excited-state geometries

1 | INTRODUCTION

Benchmark studies investigating the performance of quantum chemical methods for the calculation of electronically excited states of molecular systems usually focus on excitation energies.[1–21] At the same time, the ability of theoretical methods to provide a deep understanding of photophysical emission processes and photochemical reaction mechanisms is best explored by letting other properties of the states take center stage, such as their equilibrium geometries. However, except for small molecules,[22] reliable reference data on, for example, excited-state geometries and vibrational frequencies needed for alternative benchmarks are scarce and not easily obtained

by experimental or computational means. Although excited-state geometries can now be calculated using a wide variety of methods for which efficient implementations of analytic gradients are available,[22–38] it is of special interest to assess the performance of time-dependent density functional theory (TD-DFT)[39–46] for such calculations, as this is the most popular approach to the modeling of excited states in present-day quantum chemistry.

In a pioneering study on this topic, Furche and Ahlrichs[22] investigated how well TD-DFT reproduces experimental excited-state geometries of 24 small (2–4 atoms) inorganic and organic molecules deducible from vibrationally resolved gas-phase fluorescence spectra. Thereby, they found the calculated geometries of these systems to differ quite marginally from one density functional to another and, in many cases, the experimental bond lengths to be reproducible to within 0.01–0.02 Å.[22] These conclusions were later reinforced by Liu et al,[35] who employed the B3LYP[47–49] global hybrid and the ωB97[50] range-separated hybrid functionals to calculate TD-DFT geometries for the same benchmark set of small molecules. Specifically, these authors reported mean absolute errors (MAEs) of 0.014 (B3LYP) and 0.017 Å (ωB97) relative to the experimental bond lengths.[35]

Focusing on formal C—C single and C═C and C═O double bonds in the lowest ππ* and nπ* excited states of five small (4–5 heavy atoms) organic molecules, Guareschi and Filippi[51] instead evaluated the accuracy of TD-DFT using geometries determined through variational Monte Carlo (VMC)[52,53] calculations as reference (notably, these geometries were shown to be close to those determined by the high-level correlated CASPT2[54] and NEVPT2[55,56] methods[51]). Testing the B3LYP, PBE0,[57] and M06-2X[58] global hybrid and the CAM-B3LYP[59] and LC-BLYP[60] range-separated hybrid functionals, one particularly interesting observation in this study was that all of these methods yield C═O bond lengths in nπ* states that are too short relative to the VMC results, in some cases by up to 0.05 Å.[51] However, from the study as a whole, it was not possible to reach any clear conclusion as to which functional should be preferred over the other.

In a related study, Guido et al[61] also explored how well the lengths of formal single (C—C) and double (C═C, C═O, and C═N) bonds in low-lying ππ* and nπ* excited states of small organic molecules are reproduced by TD-DFT, but using CASPT2 data as reference. Performing calculations with five global hybrids (B3LYP, B3P86,[48,62] BH&HLYP,[47,63] PBE0 and BMK[64]) and one range-separated hybrid (CAM-B3LYP), they found the results to be more sensitive to the bond type, with MAEs ranging from 0.010–0.021 Å for C═C bonds to 0.031–0.038/0.063–0.082 Å for polar C═N/C═O bonds, than to the choice of functional.[61]

More recently, Brémond et al[65] reported the first extensive assessment of the accuracy of TD-DFT for geometries of small organic molecules in valence excited states. Testing a panel of 48 different functionals and using geometries previously calculated[66] with CASPT2 or a high-order coupled cluster (CC) method (CC3[67] or CCSDR(3)[68]) as reference, these authors concluded that excited-state bonds lengths obtained with TD-DFT are on average of somewhat lesser quality than the corresponding DFT ground-state bond lengths.[65] Consistent with the above-described findings,[51,61] this effect was manifested especially through an underestimation of C═O excited-state bond lengths.[65]

As for benchmarks focused on TD-DFT geometries of medium-sized organic molecules, which have not been the subject of many studies, Bousquet et al[69] reported overall reasonable (but system-dependent) agreement between TD-PBE0 and the SAC-CI[26,70] method in predicting excited-state geometries of nine heteroaromatic compounds. In another study, Guido et al[71] looked at bond length alternation in excited states of eight conjugated systems, comparing TD-DFT results (B3LYP, PBE0, and CAM-B3LYP) with those obtained with the approximate coupled-cluster singles and doubles (CC2)[72] method. Thereby, it was noted that the best reproduction of CC2 data is achieved by CAM-B3LYP.[71] Finally, in a study comparing excited-state geometries of 32 medium-sized organic molecules as calculated with CC2, TD-B3LYP, and two orthogonalization-corrected semiempirical methods, Tuna et al[73] documented MAEs for TD-B3LYP relative to CC2 of 0.003 (CH), 0.004 (NH), 0.011 (CC), 0.020 (CN), and 0.038 Å (CO) (this analysis includes CC, CN, and CO bonds with different bond orders).

From the survey above, it is clear that a benchmark investigating the accuracy of TD-DFT for excited-state geometries of medium-sized organic molecules using several different density functionals is still missing. Accordingly, it is the aim of this work to carry out such a study. However, the present work also has a few other notable characteristics with respect to previous works on the topic of TD-DFT geometries. The first is that the assessment is carried out in a particular two-pronged way, whereby the accuracy of calculated TD-DFT geometries is probed both through a comparison with a higher-level reference method, and through a comparison with how well DFT performs relative to the very same reference method for the *ground-state geometries* of the molecules considered.

A second key feature of our work relates to the very selection of the reference method/geometries. Specifically, for a study concerned with medium-sized systems, reference geometries are not readily available from experiments, although it should be pointed out that vibrational normal modes probed by resonance Raman spectroscopy contain information on the differences between ground- and excited-state geometries.[74–79] Therefore, the quality of reference geometries obtained computationally needs to be ascertained, either by performing the calculations with a quantitatively accurate method in combination with a large basis set (which may be too costly), or by some other means. Herein, we meet this challenge by focusing on 20 systems selected from a benchmark set of organic molecules assembled by Hättig and co-workers,[15] for which large-basis-set CC2 calculations reproduce experimentally available adiabatic excitation energies (ΔE_{00}) in the gas phase very well (MAE of 0.10 eV, see further Section 3.1) and much more closely than analogous TD-DFT calculations do (MAEs of 0.18 – 0.41 eV). Since ΔE_{00} energies are energy differences between ground and excited states at their respective equilibrium geometries, with inclusion of zero-point vibrational energy (ZPVE) corrections, the fact that CC2 yields much more

accurate ΔE_{00} energies than TD-DFT makes it sensible to adopt the corresponding excited-state geometries as reference for the TD-DFT geometries calculated in this work.

A third distinguishing characteristic of this work is that it considers a fairly large set of structural parameters: 336 bond lengths in 20 medium-sized organic molecules. Given that all of these molecules are heterocyclic or substituted aromatic compounds whose bright singlet excited states under investigation have quite uniform character, our calculations will provide a statistically sound assessment of how well TD-DFT performs for excited-state geometries of the important class of organic chromophores that these compounds represent. In our opinion, this approach is preferable to an alternative approach wherein a similarly-sized benchmark set encompassing greater chemical variation between the chromophores is considered. Indeed, although perhaps offering a potentially broader picture, the latter strategy would inevitable reduce the statistical significance of the results obtained for each individual class of chromophores.

2 | COMPUTATIONAL METHODS

2.1 | Composition of the benchmark set

The 20 aromatic compounds, ranging in size from 12 atoms in tetrafluorobenzene to 24 atoms in tryptamine, and the corresponding excited states considered are listed in Table 1, with chemical structures and atom labeling given in Figures S1 and S2 of the Supporting information. For each compound/isomer, the excited state in question is the lowest singlet excited state (S_1) and originates from a one-electron excitation out of a closed-shell ground state (S_0) into a valence state with either $\pi\pi^*$ (all states except the $^1A''$ states of 2-methylpyrimidine and 5-methylpyrimidine) or $n\pi^*$ character.[15] As such, the states are ideally suited for calculation with TD-DFT methods.[44,46,80] As for types of bonds included in the benchmark set, except where otherwise noted, the covalent interactions present in the 20 molecules are hereafter denoted X–Y based exclusively on the identities X and Y of the constituting atoms, without distinguishing formal single, double, and triple bonds. This is because excited-state geometry optimization will inevitably change the bond order of many bonds, rendering single/double/triple bond designations somewhat ambiguous. With this notation, the 336 covalent interactions in the benchmark set comprise 149 C—C, 24 C—N, 20 C—O, 6 C—F, 117 C—H, 5 N—H, and 15 O—H bonds.

TABLE 1 Molecules and excited states in the benchmark set[a]

Molecule	State	Molecule	State
2-methylpyrimidine	$1^1A''$ (S_1)	*m*-fluorophenol, *trans*	$2^1A'$ (S_1)
5-methylpyrimidine	$1^1A''$ (S_1)	Phenylacetylene	1^1B_2 (S_1)
7-azaindole	$2^1A'$ (S_1)	Resorcinol, isomer 1	2^1A (S_1)
7-hydroxyquinoline, *trans*	2^1A (S_1)	Salicylic acid	$2^1A'$ (S_1)
2-hydroxyquinoline, enol	$2^1A'$ (S_1)	*m*-cresol, *cis*	2^1A (S_1)
Pyrrolo[3,2-*h*] quinoline	$2^1A'$ (S_1)	*p*-cresol	2^1A (S_1)
Tryptamine, A-ph[b]	2^1A (S_1)	1-naphthol, *cis*	2^1A (S_1)
Tetrafluorobenzene	1^1B_1 (S_1)	2-naphthol, *cis*	$2^1A'$ (S_1)
Benzonitrile	1^1B_2 (S_1)	5-methoxysalicylic acid	$2^1A'$ (S_1)
o-fluorophenol, *trans*	2^1A (S_1)	3P-propionic acid,[c] *gauche*	2^1A (S_1)

[a]The molecules are depicted in Figure S1 of the Supporting information. Symmetry labels reflect molecular geometries after excited-state relaxation.
[b]*Anti*-ph.
[c]3-phenyl-1-propionic acid.

Given that TD-DFT has been found to underestimate[51,61,65] and CC2 to overestimate[51,66] the lengths of formal C=O double bonds in $n\pi^*$ excited states of small molecules like acetone where C=O is the dominant chromophoric moiety, using CC2 geometries of such molecules/states as reference for TD-DFT geometries warrants caution. Herein, out of the 20 C—O bonds included in the benchmark set, 17 are formal single bonds and three are formal double bonds, occurring in salicylic acid (C8=O10, see Figure S2), 5-methoxysalicylic acid (C9=O12) and 3P-propionic acid (C9=O10). However, as can be inferred from results that will be presented in Section 3.2, inclusion of the two C=O bonds in 5-methoxysalicylic acid and 3P-propionic acid in the benchmark set is not a source of concern, likely because the S_1 states of these molecules have $\pi\pi^*$ character and utilize benzene as the dominant chromophoric moiety. Regarding salicylic acid, in turn, the analysis in Section 3.2 will pay particular attention to exaggerated discrepancies between the TD-DFT and CC2 results for this compound.

2.2 | Electronic structure methods

The excited-state equilibrium geometries of the molecules in the benchmark set were optimized using TD-DFT, the CC2[72] method and, for comparative purposes, the configuration interaction singles (CIS)[24] method. Similarly, the corresponding ground-state equilibrium geometries were optimized with DFT, CC2, and the Hartree–Fock (HF) method. Employing analytic gradient techniques,[24,30,33,81] all optimizations were done with the large correlation-consistent aug-cc-pVTZ basis set,[82,83] which includes diffuse functions on all atoms. The CC2 calculations were performed within the resolution-of-the-identity (RI) approximation,[84–86] using an auxiliary aug-cc-pVTZ basis set[87] for density fitting.

The DFT and TD-DFT optimizations were carried out with six different density functionals—BP86,[62,88] B3LYP,[47–49] PBE0,[57] M06-2X,[58] CAM-B3LYP,[59] and ωB97XD[50,89]—based on the generalized gradient approximation (GGA) and belonging to different rungs of "Jacob's ladder".[90] Since many TD-DFT benchmarks have found that these functionals typically yield reliable excitation

energies,[4,6,7,9,11,12,14,19] it is of particular interest to also assess how well they perform for excited-state geometries. Briefly, BP86 is a pure GGA that lacks exact HF exchange; B3LYP and PBE0 are global hybrid GGAs that contain a fixed fraction of HF exchange (20 and 25%, respectively); M06-2X (54%) is a global hybrid meta-GGA that additionally include a dependence on the kinetic energy density; and CAM-B3LYP and ωB97XD are range-separated hybrid GGAs that contain variable fractions of HF exchange (19–65% and 22–100%, respectively) depending on the interelectronic distance: smaller at small distances and larger at large distances.

Although CAM-B3LYP and ωB97XD have been developed with an eye toward applications to charge-transfer excited states,[50,59,89] whose energies are usually underestimated by global hybrids,[44] it is pertinent to also investigate how accurately these two functionals describe other types of excited states, such as the valence ones considered in this work. Furthermore, regarding ωB97XD, it is of interest to explore whether the capability of this functional to treat dispersion interactions, owing to the inclusion of empirical $1/R^6$ terms involving ground-state parameters (dispersion coefficients, van der Waals radii, and one damping parameter[89,91]), is compatible with good performance for excited states of compounds where such interactions are of minor importance.

Based on the optimized geometries, ground- and excited-state frequency calculations were done to both confirm that the resulting structures are minima on the respective potential energy surfaces with real vibrational frequencies only, and to obtain ZPVE corrections needed to evaluate ΔE_{00} energies as

$$\Delta E_{00} = E_{el}(S_1,\boldsymbol{R}_1) + \mathrm{ZPVE}(S_1,\boldsymbol{R}_1) - E_{el}(S_0,\boldsymbol{R}_0) - \mathrm{ZPVE}(S_0,\boldsymbol{R}_0) \quad (1)$$

where E_{el} denotes electronic energy and $\boldsymbol{R}_1/\boldsymbol{R}_0$ is the geometry (excited/ground) at which the different terms are calculated. Without exception, for any given structure the frequency calculation was carried out at the same level of theory as the preceding geometry optimization. While the DFT/TD-DFT and HF/CIS frequencies were calculated using analytic Hessians,[24,92] all ground- and excited-state CC2 frequencies were determined through numerical differentiation of analytic gradients by means of finite differences.

All calculations were done with the Gaussian 16[93] and TURBOMOLE 6.3[94,95] (for CC2 calculations with the RICC2 module[86]) suites of programs.

3 | RESULTS AND DISCUSSION

3.1 | Calculated ΔE_{00} energies

Before analyzing how well the optimized TD-DFT geometries compare to the CC2 ones, it is of interest to establish how accurately the different methods reproduce the experimental ΔE_{00} energies of the states in the benchmark set. This is done in Table 2, which presents the full set of calculated ΔE_{00} energies and the corresponding experimental values first compiled by Hättig and co-workers.[15] Besides quantifying the performance of the methods in terms of their MAEs relative to the experimental data, the statistical analysis also considers their maximum absolute errors (MaxAEs) and their mean signed errors (MSEs). From this analysis, it is clear that none of the density functionals matches the MAE and MaxAE achieved by CC2, which are only 0.10 and 0.20 eV, respectively. Paralleling the results of previous studies,[15,17–19] these values testify to the accuracy and robustness of CC2 in treating singly excited states of closed-shell organic molecules. Indeed, the values are markedly smaller than those of 0.18 and 0.34 eV shown by B3LYP, which is the best-performing functional in terms of both MAE and MaxAE, followed by PBE0 (0.20 and 0.46 eV), CAM-B3LYP (0.27 and 0.52 eV), ωB97XD (0.27 and 0.53 eV), M06-2X (0.30 and 0.56 eV), and BP86 (0.41 and 1.03 eV).

The "ranking" of the functionals afforded by the data in Table 2 reinforces the conclusion from an extensive TD-DFT benchmark focused on vertical excitation energies that global hybrids with 20–25% HF exchange offer the best performance for the calculation of valence excited states of organic molecules.[7] However, it is notable that it is only among the functionals whose MAEs and MaxAEs are larger than those of B3LYP and PBE0 with which the errors are "perfectly" systematic, meaning that the calculated ΔE_{00} energies for *all* systems are either consistently smaller (BP86) or consistently larger (CAM-B3LYP and ωB97XD) than their experimental counterparts (i.e., MAE = MSE). This observation also applies to the CIS energies, which, as expected, throughout lie well above the experimental ones (MSE = 1.04 eV).

As a complement to the statistical analysis in Table 2, it is also of interest to evaluate the predictive power of the methods as quantified through linear regression analysis between the calculated and experimental ΔE_{00} energies for all states in the benchmark set. Such analyses are reported in Figure S3 of the Supporting information. As can be seen, the best performer by some margin is again CC2, which achieves an excellent R^2 value of 0.979. Similarly, at the other end of the spectrum, the worst performers are BP86 (0.760) and CIS (0.690), which is consistent with the analysis in Table 2. However, in the intermediate R^2 range occupied by the hybrid functionals, the MAE-based ranking that places B3LYP and PBE0 ahead of CAM-B3LYP and ωB97XD, is reversed. Specifically, while the former two methods have R^2 values of 0.938 and 0.943, respectively, the latter two methods fare somewhat better with R^2 values of 0.953 and 0.954.

All in all, since ΔE_{00} energies are energy differences between ground and excited states at their equilibrium geometries, the marked difference in performance between TD-DFT and CC2 highlighted by the results in Table 2 and Figure S3 shows that it is sensible to assess the accuracy of the TD-DFT geometries calculated for the present benchmark set using the corresponding CC2 geometries as reference. Of course, the CC2 geometries are by no means "exact" and, as pointed out by Loos and Jacquemin,[21] may well contain errors that are not revealed by an analysis of ΔE_{00} energies alone. However, based on the data in Table 2 and Figure S3, the CC2 geometries appear sufficiently more accurate than the TD-DFT ones for them to enable a meaningful assessment of the latter's accuracy. Furthermore, even in the presence of inevitable errors in the CC2 geometries, comparing

TABLE 2 Calculated ΔE_{00} energies for all states in the benchmark set (in eV)[a]

		Method								
Molecule	State	BP86	B3LYP	PBE0	M06-2X	CAM-B3LYP	ωB97XD	CIS	CC2	Exp.
2-methylpyrimidine	$1^1A''$	3.19	3.60	3.68	3.73	3.87	3.84	5.17	3.67	3.78
5-methylpyrimidine	$1^1A''$	3.19	3.64	3.72	3.77	3.91	3.88	5.17	3.73	3.82
7-azaindole	$2^1A'$	3.69	4.06	4.19	4.47	4.44	4.44	5.11	4.30	4.29
7-hydroxyquinoline, *trans*	2^1A	2.95	3.50	3.59	3.75	3.87	3.83	4.77	3.83	3.78
2-hydroxyquinoline, enol	$2^1A'$	3.50	3.83	3.94	4.18	4.15	4.14	4.82	3.94	3.89
Pyrrolo[3,2-*h*]quinoline	$2^1A'$	3.17	3.48	3.61	3.86	3.91	3.93	4.54	3.65	3.66
Tryptamine, A-ph	2^1A	3.29	4.08	4.20	4.46	4.45	4.48	4.82	4.29	4.32
Tetrafluorobenzene	1^1B_1	4.32	4.67	4.82	4.91	4.87	4.86	5.78	4.60	4.53
Benzonitrile	1^1B_2	4.51	4.81	4.92	5.08	4.97	5.02	5.64	4.73	4.53
o-fluorophenol, *trans*	2^1A	4.37	4.67	4.79	4.95	4.89	4.90	5.65	4.65	4.58
m-fluorophenol, *trans*	$2^1A'$	4.52	4.79	4.91	5.03	4.98	4.98	5.84	4.71	4.57
Phenylacetylene	1^1B_2	4.32	4.66	4.76	4.99	4.96	4.95	5.22	4.65	4.45
Resorcinol, isomer 1	2^1A	4.36	4.63	4.77	4.90	4.84	4.84	5.40	4.57	4.49
Salicylic acid	$2^1A'$	3.31	3.74	3.82	4.10	4.06	4.00	5.13	3.60	3.70
m-cresol, *cis*	2^1A	4.39	4.64	4.76	4.89	4.85	4.85	5.63	4.58	4.46
p-cresol	2^1A	4.29	4.52	4.64	4.77	4.72	4.73	5.42	4.48	4.38
1-naphthol, *cis*	2^1A	3.25	3.58	3.68	3.95	3.92	3.94	4.58	3.90	3.87
2-naphthol, *cis*	$2^1A'$	3.58	3.78	3.87	4.09	4.06	4.07	4.64	3.93	3.83
5-methoxysalicylic acid	$2^1A'$	2.94	3.36	3.46	3.75	3.66	3.68	4.67	3.34	3.49
3P-propionic acid, *gauche*	2^1A	3.76	5.01	5.13	5.23	5.19	5.20	5.82	4.86	4.67
MAE[b]		0.41	0.18	0.20	0.30	0.27	0.27	1.04	0.10	–
MaxAE[b]		1.03	0.34	0.46	0.56	0.52	0.53	1.43	0.20	–
MSE[b]		−0.41	0.00	0.11	0.29	0.27	0.27	1.04	0.05	–
MAE(CC2)[c]		0.46	0.12	0.14	0.25	0.23	0.23	0.99	–	–
MaxAE(CC2)[c]		1.10	0.33	0.27	0.50	0.46	0.40	1.53	–	–
MSE(CC2)[c]		−0.46	−0.05	0.06	0.24	0.23	0.23	0.99	–	–

[a]Experimental values compiled in Reference [15], see also references therein.
[b]Mean absolute error (MAE), maximum absolute error (MaxAE) and mean signed error (MSE) relative to the experimental values for all states.
[c]Mean absolute error (MAE), maximum absolute error (MaxAE) and mean signed error (MSE) relative to the CC2 values for all states.

TD-DFT to CC2 seems worthwhile merely on account of the fact that CC2, despite its ability to capture dynamic electron correlation effects in a cost-effective manner, is a much more expensive method than TD-DFT, especially for geometry optimizations and frequency calculations.

3.2 | Calculated bond lengths: Individual molecules

Our first order of business for the comparison of the TD-DFT and CC2 excited-state bond lengths will be to assess the extent to which the outcome of this comparison varies from one molecule in the benchmark set to another. For each of the six density functionals employed (and CIS), this is done in Figure 1. Specifically, for each molecule in the benchmark set, Figure 1 plots the root mean square deviation (RMSD) of the TD-DFT bond lengths relative to the CC2 ones, calculated as

$$\mathrm{RMSD} = \sqrt{\frac{1}{N}\sum (r_i - r_{i,\mathrm{CC2}})^2} \quad (2)$$

where the sum runs over all N bonds in the molecule and r_i is a TD-DFT bond length and $r_{i,\mathrm{CC2}}$ is the corresponding CC2 bond length. In line with the purpose of the study, Figure 1 also includes a RMSD-based analysis of how well the DFT *ground-state* bond lengths compare to those obtained with CC2. The actual bond lengths of the 20 molecules calculated with the different methods are listed in Tables S1a-S20a (ground state) and S1b-S20b (excited state) of the Supporting information, which for clarity also includes the RMSD values in Figure 1 in Table S21.

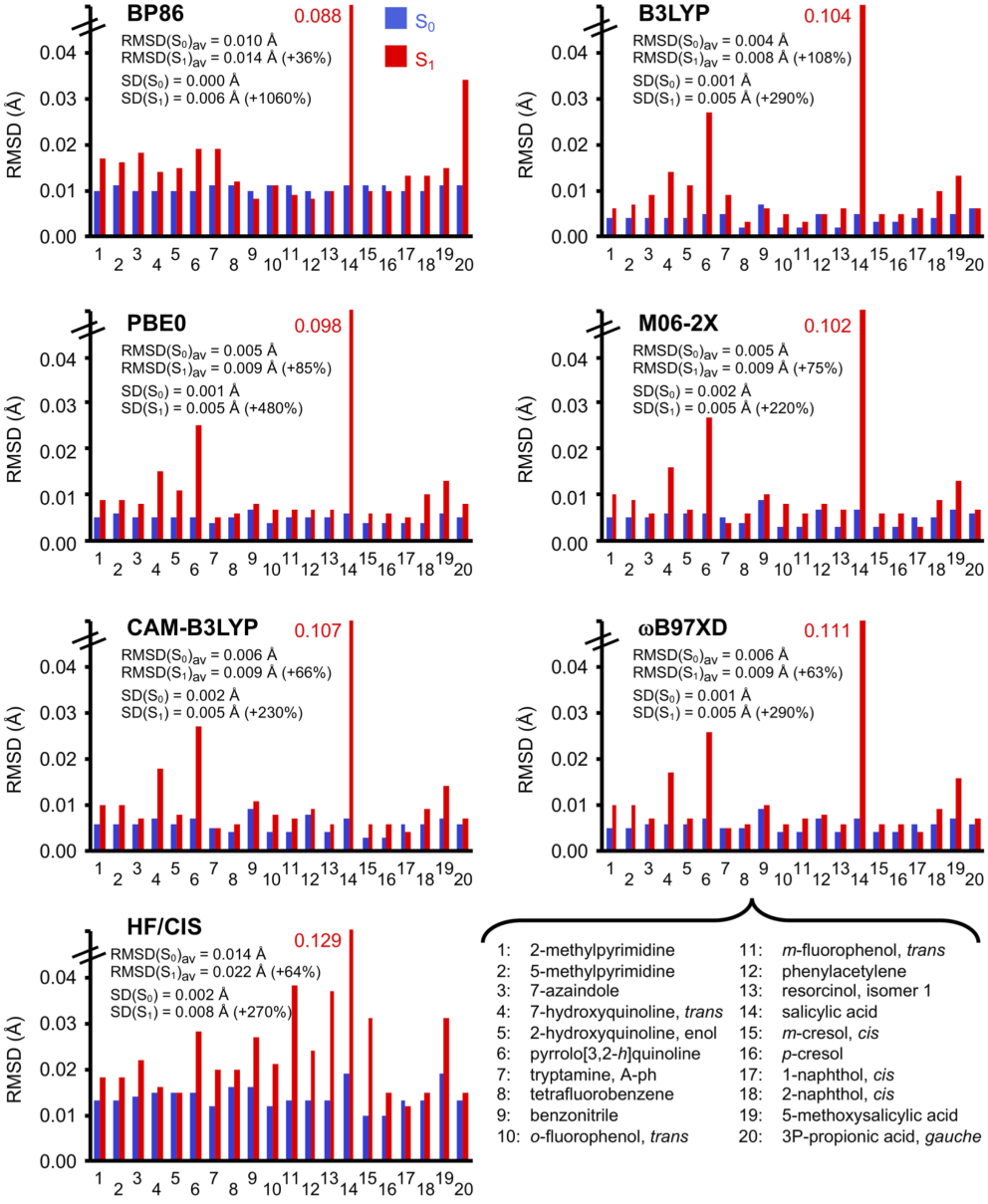

FIGURE 1 S_0 and S_1 bond-length RMSD values relative to CC2 for different methods evaluated for individual molecules in the benchmark set. Average RMSD values are denoted $RMSD(S_0)_{av}$ and $RMSD(S_1)_{av}$, standard deviations are denoted $SD(S_0)$ and $SD(S_1)$. Percentages indicate how much larger the $RMSD(S_1)_{av}$ and $SD(S_1)$ values are than the $RMSD(S_0)_{av}$ and $SD(S_0)$ values, respectively [Color figure can be viewed at wileyonlinelibrary.com]

At this point, before discussing the results in Figure 1, two issues should be commented upon. The first concerns the reference ground-state geometries, which possibly could have been derived with a better method than CC2, such as the "gold-standard" CCSD(T) method. However, using reference geometries obtained at a different level of theory for the ground state than for the excited state, would make it difficult to realize the central goal of the study to present a balanced assessment of how accurate TD-DFT excited-state geometries are compared to DFT ground-state geometries. In other words, the choice of CC2 as reference method for the excited-state geometries is the deciding factor in this regard. The second issue is ascertaining that the CC2 reference geometries are converged at the aug-cc-pVTZ basis-set level chosen for the calculations. To this end, for six representative molecules in the benchmark set (2-methylpyrimidine, 7-azaindole, benzonitrile, *m*-fluorophenol, *p*-cresol and 1-naphthol), Tables S22–S27 of the Supporting information compare CC2 bond lengths (both S_0 and S_1) obtained with the cc-pVDZ → cc-pVTZ → aug-cc-pVTZ sequence of increasingly larger basis sets. Encouragingly, the final addition of diffuse functions to the cc-pVTZ basis set is associated with very small effects on the calculated bond lengths. Indeed, for each of the six molecules and for both states, the effect never exceeds 0.003 Å. Accordingly, the CC2/aug-cc-pVTZ geometries appear well converged with respect to the choice of basis set. In this context, it may also be mentioned that this basis set has been used in several of the previous benchmarks on the topic of excited-state geometries that have included the CC2 method.[51,66,71]

The first observation that can be made in Figure 1 is that the $RMSD(S_1)$ values of ~0.09–0.11 Å uniformly shown by the different density functionals for salicylic acid vastly exceed the $RMSD(S_1)$ values of ~0.01 Å that these methods exhibit for most of the other

molecules. As can be inferred from the S_0 and S_1 bond lengths of salicylic acid in Tables S14a and S14b, this is because CC2—but none of the density functionals—predicts a transfer of the H15 proton (see Figure S2) from O7 to O10 when salicylic acid is promoted to the excited state. For this reason, when later turning to the RMSD values for different types of bonds (see Section 3.3), the analysis will exclude the C2—O7, C8—O9, C8—O10, and O7—H15 bonds in salicylic acid. It appears likely that this discrepancy between TD-DFT and CC2, which has also been documented in studies of excited-state intramolecular proton transfer reactions in other compounds similar to salicylic acid,[96] relates to the aforementioned tendencies of TD-DFT to underestimate and CC2 to overestimate the lengths of formal C═O double bonds in excited states,[51,61,65,66] although these tendencies have mostly been manifested in studies of $n\pi^*$ states of small molecules where C═O is the main chromophoric moiety.

A second key observation in Figure 1 concerns the RMSD(S_1) values shown by the functionals for 5-methoxysalicylic acid and 3P-propionic acid, both of which also feature a formal C═O double bond (C9═O12 and C9═O10, respectively, see Figure S2). Notably, however, the corresponding TD-DFT bond lengths fall in ranges that are not indicative of a systematic underestimation vis-à-vis the CC2 bond lengths. Specifically, as can be seen from Tables S19b and S20b, the TD-DFT bond lengths of 1.250–1.277 (for C9—O12 in 5-methoxysalicylic acid) and 1.201–1.299 Å (for C9—O10 in 3P-propionic acid) are not distinctly smaller than the corresponding CC2 bond lengths of 1.279 and 1.217 Å, respectively. Furthermore, although Figure 1 shows that BP86 has a large RMSD(S_1) value of 0.034 Å for 3P-propionic acid, this is chiefly because this method predicts a much *longer* C9—O10 bond in the excited state (1.299 Å) than both CC2 (1.217 Å) and the other functionals (1.201–1.209 Å).

From Figure 1, it is also interesting to note that although the average (over all molecules) RMSD(S_1) values for the different functionals are small, ranging from 0.008–0.009 (all hybrid functionals) to 0.014 Å (BP86), they consistently exceed the average RMSD(S_0) values, which fall between 0.004–0.006 (all hybrid functionals) and 0.010 Å (BP86). More precisely, depending on the functional, the average RMSD(S_1) value is 36–108% larger than the average RMSD(S_0) value. Thus, while TD-DFT reproduces the CC2 excited-state bond lengths rather well, the agreement is not comparable to that between DFT and CC2 for the ground-state bond lengths. To the best of our knowledge, this is the first time that the accuracy of TD-DFT for excited-state geometries of medium-sized organic molecules is assessed in this two-pronged way, including not only the customary comparison with a higher-level reference method, but also a direct comparison with how DFT performs relative to the very same reference method for the ground-state geometries of the molecules in question.

Another notable difference between the RMSD(S_0) and RMSD(S_1) values in Figure 1 is that the latter vary much more between the different molecules in the benchmark set than the former. Specifically, evaluating the standard deviations (SDs) in the calculated RMSD values as (where the sum runs over all M molecules except salicylic acid, and $RMSD_{av}$ is the average RMSD value)

$$SD = \sqrt{\frac{1}{M}\sum (RMSD_i - RMSD_{av})^2} \quad (3)$$

the variation in the RMSD(S_1) values is for each functional found to be at least a factor of 3 larger (i.e., 200% larger) than that in the RMSD(S_0) values. Hence, the performance of any given functional—as evaluated relative to CC2—depends much more strongly on the chemical system studied for excited-state geometries than for ground-state geometries. In other words, even for the present set of chemically and spectroscopically similar organic molecules/states, the challenge to obtain geometries of uniform quality is far greater at the TD-DFT level than at the DFT level. As best we know, no previous benchmark study has probed the magnitude of this effect in a similarly direct and quantitative fashion.

Having already highlighted that all functionals exhibit their largest RMSD(S_1) value for salicylic acid, it can also be seen from Figure 1 that the two molecules for which all *hybrid* functionals show their second and third largest RMSD(S_1) values are pyrrolo[3,2-*h*]quinoline (~0.03 Å) and 7-hydroxyquinoline (~0.02 Å). As can be deduced from the S_1 bond lengths in Table S6b, the sizable RMSD(S_1) values for pyrrolo[3,2-*h*]quinoline are largely attributable to the prediction by the hybrid functionals that the C17—N18 bond (see Figure S2) is noticeably longer than the C10—N18 bond in the excited state (1.395–1.408 vs. 1.331–1.336 Å), which is qualitatively opposite to the prediction by CC2 (1.348 vs. 1.378 Å). No such difference between the hybrid functionals and CC2 is manifested in the descriptions of these bonds in the ground state (see Table S6a), with all methods yielding a slightly longer C17—N18 bond and with all hybrid functionals reproducing the CC2 bond lengths to within 0.006 (C17—N18) and 0.007 Å (C10—N18). Regarding 7-hydroxyquinoline, in turn, the magnitudes of the RMSD(S_1) values shown by the hybrid functionals are also primarily due to a discrepancy between these methods and CC2 in calculated C—N bond lengths. Specifically, as revealed by the data in Table S4b, the hybrid functionals consistently yield shorter C2—N1 (by up to 0.025 Å) and C6—N1 (by up to 0.038 Å) bond lengths than CC2.

3.3 | Calculated bond lengths: Different types of bonds

We now move on to analyze the RMSD(S_0) and RMSD(S_1) values that the different density functionals show when the comparison with the CC2 bond lengths extends over all 336 bonds in the benchmark set, or is made over all bonds of a given type (C—C, C—N, C—O, C—F, C—H, N—H, or O—H) in the benchmark set. This is done in Figure 2, with precise numerical values and further information given in Table S28 of the Supporting information. Starting with the RMSD(S_1) values evaluated over all 336 bonds, the differences in performance between the hybrid functionals are virtually negligible, with each of B3LYP, PBE0, M06-2X, CAM-B3LYP and ωB97XD achieving an accuracy of 0.011 Å relative to CC2 (the corresponding BP86 value is

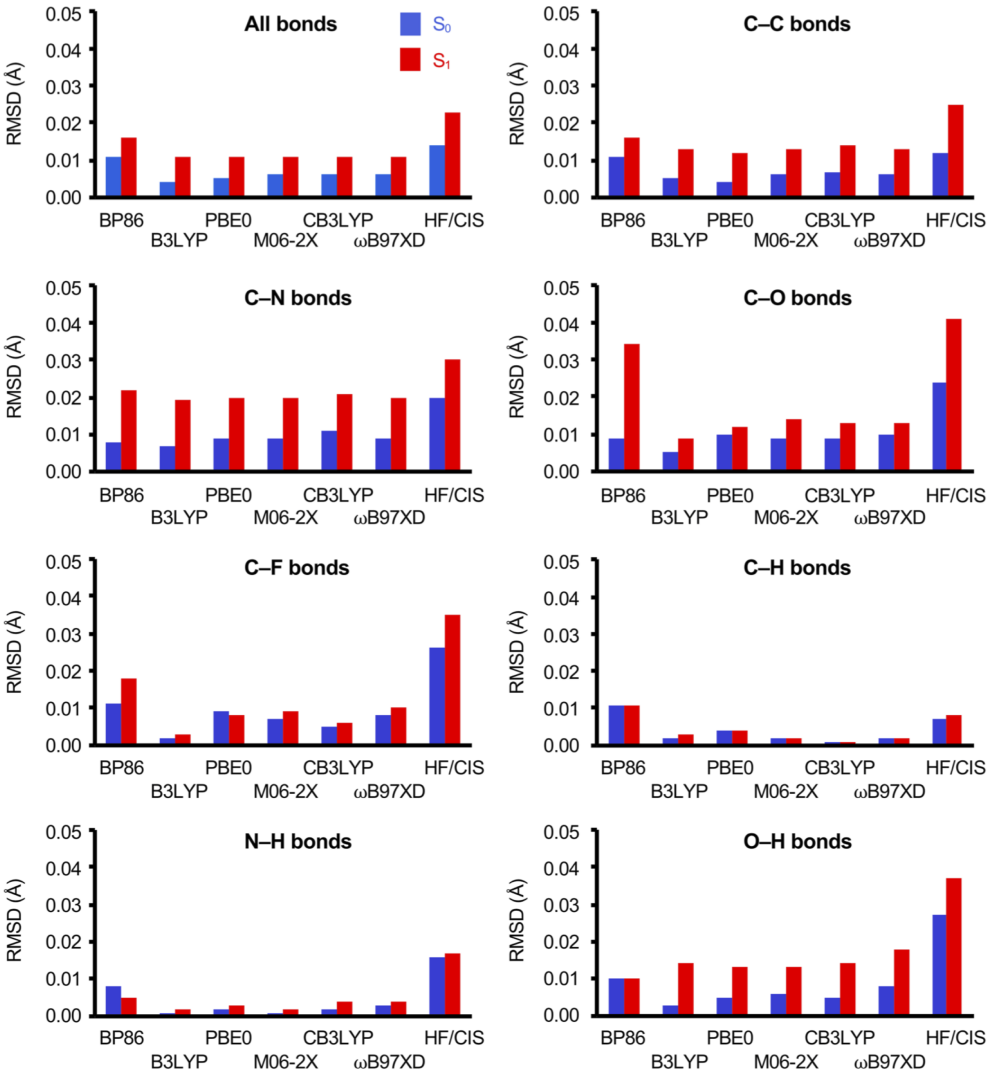

FIGURE 2 S_0 and S_1 bond-length RMSD values relative to CC2 for different methods evaluated over all bonds in the benchmark set and over all bonds of a given type in the benchmark set. See text for further information. CAM-B3LYP is denoted CB3LYP [Color figure can be viewed at wileyonlinelibrary.com]

worse, 0.016 Å). These results parallel the observation in Figure 1 that the average RMSD(S_1) values for the hybrid functionals over individual molecules fall in a narrow 0.008–0.009 Å range. Also, the 0.011 Å accuracy is similar to that of 0.009 Å found by Brémond et al[65] for the best-performing functionals in their extensive benchmark on TD-DFT geometries of small organic molecules.

Noting from Table 2 that the MAEs in the ΔE_{00} energies of the hybrid functionals relative to CC2 vary from 0.12 to 0.25 eV (these MAEs complement the MAEs relative to experiment already discussed in Section 3.2), it appears clear from a statistical viewpoint that the dependence on the choice of hybrid functional is much less pronounced for the calculation of excited-state geometries than for the calculation of ΔE_{00} energies. As an aside, the MAE-based ranking of the functionals according to the accuracy in their ΔE_{00} energies relative to CC2 is exactly the same as that according to the accuracy in their ΔE_{00} energies relative to the experimental values, with the smallest MAE achieved by B3LYP (0.12 eV), followed by PBE0 (0.14 eV), CAM-B3LYP/ωB97XD (0.23 eV), M06-2X (0.25 eV), and BP86 (0.46 eV).

Continuing with the RMSD(S_1) values evaluated over the full benchmark set, but now assessing them in relation to the corresponding RMSD(S_0) values, Figure 2 reaffirms that although the hybrid functionals on the whole reproduce the CC2 excited-state bond lengths very satisfactorily (RMSD(S_1) = 0.011 Å), their accuracy is still not comparable to that with which they reproduce the CC2 ground-state bond lengths (RMSD(S_0) = 0.004–0.006 Å). Importantly, this finding also applies to each of the C—C, C—N, C—O, C—F, C—H, N—H, and O—H subgroups of the benchmark set. Notably, the overall RMSD(S_0) values of 0.004–0.006 Å are comparable to the MAEs of ~0.005 Å documented for the best-performing functionals in a previous extensive benchmark investigating the accuracy of DFT for ground-state geometries of small and medium-sized organic molecules,[97] using CCSD(T) data as reference.[98] As an aside, and given that it has proven difficult to assign a value to the range-separation parameter employed by the CAM-B3LYP and ωB97XD hybrids that is suitable for excited states whilst simultaneously also enabling an accurate description of ground-state properties,[99] it is noteworthy that these two functionals perform almost just as well for

the ground-state bond lengths as the B3LYP and PBE0 global hybrids do.

As a further test of whether the default values of the range-separation parameter of CAM-B3LYP (0.33 $Bohr^{-1}$)[59] and ωB97XD (0.20 $Bohr^{-1}$)[89] are appropriate for the task at hand, these functionals and B3LYP were used to calculate ionization potentials (IPs) for the 20 molecules in the benchmark set in two different ways: (a) as the vertical energy difference between the ionized and parent species, and (b) as the negative of the energy of the highest occupied molecular orbital of the parent species ($-\varepsilon_{HOMO}$). In principle, and in accordance with Koopmans' theorem in HF theory, the latter approach should be a reasonable approximation to the former, provided that the functionals meet certain criteria.[100,101] Denoting the corresponding IPs as VIP and KIP, respectively, the results of these calculations are summarized in Figure S4 of the Supporting information. As expected,[99] at the reference B3LYP level without any range-separation, the KIP values are noticeably smaller than the VIP values, by on average 1.97 eV. However, with CAM-B3LYP and ωB97XD, the agreement between the two approaches is much improved, reaching on average 0.68 (CAM-B3LYP) and 0.12 eV (ωB97XD). Thereby, the default values of the range-separation parameter used by these functionals seem suitable.

Moving on to the RMSD(S_1) values obtained for the different types of bonds, Figure 2 shows that the results for the C—C bonds essentially mirror the results for the full benchmark set. Specifically, all the hybrid functionals have similar RMSD(S_1) values somewhat smaller (0.012–0.014 Å) than that of BP86 (0.016 Å). For the C—H bonds, in turn, the hybrid functionals have RMSD(S_1) values of a mere 0.001–0.004 Å, and thus achieve near-perfect agreement with the CC2 excited-state bond lengths. In contrast, the corresponding BP86 value is larger, 0.011 Å. Continuing with the results for the polar bonds, it is firstly interesting to note that the RMSD(S_1) values of 0.009–0.014 Å that the hybrid functionals show for the C—O bonds are similar to the values of 0.012–0.014 Å that they show for the C—C bonds. Accordingly, having already seen in Section 3.2 that the tendency of TD-DFT to underestimate and CC2 to overestimate the lengths of formal C═O double bonds (observed in studies of nπ* states of small molecules[51,61,65,66]) is *not* generally manifested in the descriptions by hybrid functionals of such bonds, it appears clear that this tendency is of no immediate consequence for the descriptions of formal C—O single bonds either (recalling here that all C—O bonds in the benchmark set except C8═O10 in salicylic acid, C9═O12 in 5-methoxysalicylic acid and C9═O10 in 3P-propionic acid are nominally single bonds). While the BP86 RMSD(S_1) value for the C—O bonds is large (0.034 Å), this is primarily because this functional *overestimates* the C9—O10 and C9—O11 bond lengths in 3P-propionic acid by a whopping 0.08–0.09 Å relative to CC2 (see Table S20b).

In contrast to the results for the C—O bonds just described, for the C—N bonds the hybrid functionals have somewhat larger RMSD(S_1) values (0.019–0.021 Å) than they have for the C—C bonds (0.012–0.014 Å), as clearly seen in Figure 2. This finding is consistent with the results of Tuna et al,[73] who tested the performance of two semiempirical methods and a single hybrid functional (B3LYP) in reproducing the CC2 excited-state geometries of organic molecules, and found MAEs for B3LYP of 0.020 Å for C—N bonds and 0.011 Å for C—C bonds.[73] Similar to the present work, the analyses in that study did not distinguish between C—C, C—N, and C—O bonds with different bond orders. However, one notable difference between the two studies is that Tuna et al[73] reported much poorer agreement between B3LYP and CC2 for C—O bonds (MAE = 0.038 Å) than for C—N bonds (MAE = 0.020 Å), whereas B3LYP and all other hybrid functionals employed in the present work show *smaller* RMSD(S_1) values for the C—O bonds (0.009–0.014 Å) than for the C—N bonds (0.019–0.021 Å). One likely explanation for this discrepancy is that among the systems studied by Tuna et al[73] are several nπ* states of small molecules such as formaldehyde, acetaldehyde and acetone for which, as noted above, TD-DFT and CC2 respectively overbinds and underbinds formal C═O double bonds,[51,61,65,66] possibly due to an underestimation/overestimation of electron correlation effects by TD-DFT/CC2.[102] In the present work, on the other hand, 18 of the 20 excited states studied are ππ* states and neither of the two nπ* states considered is associated with a C═O moiety, corresponding as they do to the $^1A''$ states of 2-methylpyrimidine and 5-methylpyrimidine.

Assessing, finally, the RMSD(S_1) values for the C—F, N—H, and O—H bonds in Figure 2, it should be recalled that only six C—F and five N—H bonds are included in the benchmark set. With this caveat in mind, neither of these three subgroups of bonds seems to pose a greater challenge for TD-DFT modeling than the four subgroups already discussed (i.e., C—C, C—N, C—O, and C—H). For example, both BP86 and the hybrid functionals show RMSD(S_1) values for the C—F bonds that are smaller than the ones for the C—N and C—O bonds.

4 | CONCLUSIONS

In summary, using six different density functionals (BP86, B3LYP, PBE0, M06-2X, CAM-B3LYP, and ωB97XD), we have investigated how well the S_1 geometries of 20 heterocyclic or substituted aromatic compounds calculated with TD-DFT compare to those calculated with the CC2 method. This endeavor is motivated both by the scarcity in the existing literature of TD-DFT benchmark studies focused on excited-state geometries of medium-sized organic molecules, and by the fact that CC2 is generally a much more precise, robust, and expensive method than TD-DFT.[15,17–19]

From the calculations, it is found that the B3LYP, PBE0, M06-2X, CAM-B3LYP, and ωB97XD hybrid functionals reproduce the CC2 excited-state bond lengths very satisfactorily, with each functional achieving an overall (for all 336 bonds in the benchmark set) RMSD relative to CC2 of 0.011 Å only. At the same time, this accuracy is noticeably worse than that with which the functionals reproduce the corresponding CC2 ground-state bond lengths, which translates into RMSD values of a mere 0.004–0.006 Å. Thus, even for a benchmark set like the present one consisting of low-lying singly excited valence states ideally suited for TD-DFT modeling, the performance of conventional TD-DFT (e.g., invoking the adiabatic approximation[80]) for

excited-state geometries is not comparable to that of DFT for ground-state geometries. Furthermore, for each functional employed, it is also found that the variation in the RMSD error from one molecule in the benchmark set to another is much larger for the excited-state geometries than for the ground-state geometries—in terms of the associated SDs and depending on the functional used, the variation is at least three times larger for the former geometries. Hence, given the chemical and spectroscopic similarity of the molecules/states under investigation, there seems to be an intrinsic—but hitherto unquantified—difference in the abilities of DFT and TD-DFT to produce molecular structures of uniform quality. All in all, the calculations support the conclusion that TD-DFT geometries are comparatively less accurate than DFT ones, even in favorable circumstances.

As for the performance of TD-DFT relative to CC2 for the different types of bonds in the benchmark set, the aforementioned hybrid functionals are found to have the largest RMSD errors for C—N bonds, whose values of 0.019–0.021 Å can be compared with the corresponding errors of 0.011 Å over *all* bonds in the benchmark set. A comparison can also be made with the RMSD errors of 0.009–0.014 Å for the description of C—O bonds, whose smallness suggests that the difficulty in reconciling the descriptions by TD-DFT and CC2 of such bonds in $n\pi^*$ excited states[51,61,65,66] is of minor consequence for the $\pi\pi^*$ excited states that predominantly make up the current benchmark set.

As for identifying a preferred functional for TD-DFT calculation of excited-state geometries, which has not been the primary motivation for our work, the present results strongly favor hybrid functionals over BP86. However, singling out a preferred hybrid is less straightforward, since each of them achieves an overall RMSD relative to CC2 of 0.011 Å (the corresponding BP86 value is 0.016 Å). Notwithstanding, if particular significance is attributed to the description of C—C, C—N and C—O bonds, then none of the M06-2X, CAM-B3LYP, and ωB97XD hybrids performs better than B3LYP and PBE0. Combined with the fact that B3LYP and PBE0 are widely used methods for calculating ground-state geometries, and herein indeed show the smallest overall RMSD errors relative to the CC2 ground-state geometries, the recommendation from this work is therefore that B3LYP and PBE0 are suitable functionals for TD-DFT calculation of excited-state geometries.

Finally, we note that a natural goal of future work aimed at further establishing the accuracy of TD-DFT for excited-state geometries is to include among the target systems molecules taking center stage in many fertile areas of current photochemical modeling, such as transition-metal compounds,[103,104] chromophores of photosensory proteins,[105,106] and molecular photoswitches.[107–109] Moreover, it is also of interest to bring the benchmarking of excited-state calculations beyond properties like excitation energies and molecular geometries, toward properties that better reflect the character and chemical reactivity of excited states. Initial work along those lines includes an insightful study focused on exciton properties[110] and assessments of how accurately TD-DFT reproduces experimental free-energy barriers and equilibrium constants of excited-state intramolecular proton transfer reactions.[111,112]

ACKNOWLEDGMENTS

We gratefully acknowledge financial support from Linköping University, the Olle Engkvist Foundation (grant 184-568) and the Swedish Research Council (grant 2019-03664), as well as grants of computing time at the National Supercomputer Centre (NSC) in Linköping.

ORCID

Jun Wang https://orcid.org/0000-0003-0222-6380
Bo Durbeej https://orcid.org/0000-0001-5847-1196

REFERENCES

[1] D. J. Tozer, R. D. Amos, N. C. Handy, B. O. Roos, L. Serrano-Andrés, *Mol. Phys.* **1999**, *97*, 859.
[2] C.-P. Hsu, S. Hirata, M. Head-Gordon, *J. Phys. Chem. A.* **2001**, *105*, 451.
[3] S. Grimme, E. I. Izgorodina, *Chem. Phys.* **2004**, *305*, 223.
[4] D. Jacquemin, E. A. Perpète, G. E. Scuseria, I. Ciofini, C. Adamo, *J. Chem. Theory Comput.* **2008**, *4*, 123.
[5] M. Schreiber, M. R. Silva-Junior, S. P. A. Sauer, W. Thiel, *J. Chem. Phys.* **2008**, *128*, 134110.
[6] M. R. Silva-Junior, M. Schreiber, S. P. A. Sauer, W. Thiel, *J. Chem. Phys.* **2008**, *129*, 104103.
[7] D. Jacquemin, V. Wathelet, E. A. Perpète, C. Adamo, *J. Chem. Theory Comput.* **2009**, *5*, 2420.
[8] S. P. A. Sauer, M. Schreiber, M. R. Silva-Junior, W. Thiel, *J. Chem. Theory Comput.* **2009**, *5*, 555.
[9] M. Caricato, G. W. Trucks, M. J. Frisch, K. B. Wiberg, *J. Chem. Theory Comput.* **2010**, *6*, 370.
[10] L. Goerigk, S. Grimme, *J. Chem. Phys.* **2010**, *132*, 184103.
[11] R. Send, M. Kühn, F. Furche, *J. Chem. Theory Comput.* **2011**, *7*, 2376.
[12] S. S. Leang, F. Zahariev, M. S. Gordon, *J. Chem. Phys.* **2012**, *136*, 104101.
[13] M. Uppsten, B. Durbeej, *J. Comput. Chem.* **2012**, *33*, 1892.
[14] D. Jacquemin, A. Planchat, C. Adamo, B. Mennucci, *J. Chem. Theory Comput.* **2012**, *8*, 2359.
[15] N. O. C. Winter, N. K. Graf, S. Leutwyler, C. Hättig, *Phys. Chem. Chem. Phys.* **2013**, *15*, 6623.
[16] D. Jacquemin, B. Moore II, A. Planchat, C. Adamo, J. Autschbach, *J. Chem. Theory Comput.* **2014**, *10*, 1677.
[17] C. Fang, B. Oruganti, B. Durbeej, *J. Phys. Chem. A* **2014**, *118*, 4157.
[18] D. Jacquemin, I. Duchemin, X. Blase, *J. Chem. Theory Comput.* **2015**, *11*, 5340.
[19] B. Oruganti, C. Fang, B. Durbeej, *Mol. Phys.* **2016**, *114*, 3448.
[20] P.-F. Loos, N. Galland, D. Jacquemin, *J. Phys. Chem. Lett.* **2018**, *9*, 4646.
[21] P.-F. Loos, D. Jacquemin, *J. Chem. Theory Comput.* **2019**, *15*, 2481.
[22] F. Furche, R. Ahlrichs, *J. Chem. Phys.* **2002**, *117*, 7433.
[23] Y. Osamura, Y. Yamaguchi, H. F. Schaefer III, *J. Chem. Phys.* **1982**, *77*, 383.
[24] J. B. Foresman, M. Head-Gordon, J. A. Pople, M. J. Frisch, *J. Phys. Chem.* **1992**, *96*, 135.
[25] J. F. Stanton, J. Gauss, *J. Chem. Phys.* **1994**, *100*, 4695.
[26] T. Nakajima, H. Nakatsuji, *Chem. Phys. Lett.* **1997**, *280*, 79.
[27] S. R. Gwaltney, R. J. Bartlett, *J. Chem. Phys.* **1999**, *110*, 62.
[28] C. Van Caillie, R. D. Amos, *Chem. Phys. Lett.* **2000**, *317*, 159.
[29] H. Lischka, M. Dallos, R. Shepard, *Mol. Phys.* **2002**, *100*, 1647.
[30] A. Köhn, C. Hättig, *J. Chem. Phys.* **2003**, *119*, 5021.
[31] P. Celani, H.-J. Werner, *J. Chem. Phys.* **2003**, *119*, 5044.
[32] S. V. Levchenko, T. Wang, A. I. Krylov, *J. Chem. Phys.* **2005**, *122*, 224106.

[33] G. Scalmani, M. J. Frisch, B. Mennucci, J. Tomasi, R. Cammi, V. Barone, *J. Chem. Phys.* **2006**, *124*, 094107.
[34] M. Chiba, T. Tsuneda, K. Hirao, *J. Chem. Phys.* **2006**, *124*, 144106.
[35] F. Liu, Z. Gan, Y. Shao, C.-P. Hsu, A. Dreuw, M. Head-Gordon, B. T. Miller, B. R. Brooks, J.-G. Yu, T. R. Furlani, J. Kong, *Mol. Phys.* **2010**, *108*, 2791.
[36] N. O. C. Winter, C. Hättig, *Chem. Phys.* **2012**, *401*, 217.
[37] W. Győrffy, T. Shiozaki, G. Knizia, H.-J. Werner, *J. Chem. Phys.* **2013**, *138*, 104104.
[38] M. G. Delcey, L. Freitag, T. B. Pedersen, F. Aquilante, R. Lindh, L. González, *J. Chem. Phys.* **2014**, *140*, 174103.
[39] E. Runge, E. K. U. Gross, *Phys. Rev. Lett.* **1984**, *52*, 997.
[40] M. Petersilka, U. J. Gossmann, E. K. U. Gross, *Phys. Rev. Lett.* **1996**, *76*, 1212.
[41] R. Bauernschmitt, R. Ahlrichs, *Chem. Phys. Lett.* **1996**, *256*, 454.
[42] R. E. Stratmann, G. E. Scuseria, M. J. Frisch, *J. Chem. Phys.* **1998**, *109*, 8218.
[43] M. A. L. Marques, E. K. U. Gross, *Annu. Rev. Phys. Chem.* **2004**, *55*, 427.
[44] A. Dreuw, M. Head-Gordon, *Chem. Rev.* **2005**, *105*, 4009.
[45] M. E. Casida, *J. Mol. Struct. THEOCHEM* **2009**, *914*, 3.
[46] M. E. Casida, M. Huix-Rotllant, *Annu. Rev. Phys. Chem.* **2012**, *63*, 287.
[47] C. Lee, W. Yang, R. G. Parr, *Phys. Rev. B* **1988**, *37*, 785.
[48] A. D. Becke, *J. Chem. Phys.* **1993**, *98*, 5648.
[49] P. J. Stephens, F. J. Devlin, C. F. Chabalowski, M. J. Frisch, *J. Phys. Chem.* **1994**, *98*, 11623.
[50] J.-D. Chai, M. Head-Gordon, *J. Chem. Phys.* **2008**, *128*, 084106.
[51] R. Guareschi, C. Filippi, *J. Chem. Theory Comput.* **2013**, *9*, 5513.
[52] O. Valsson, C. Filippi, *J. Chem. Theory Comput.* **2010**, *6*, 1275.
[53] B. M. Austin, D. Y. Zubarev, W. A. Lester Jr., *Chem. Rev.* **2012**, *112*, 263.
[54] K. Andersson, P.-Å. Malmqvist, B. O. Roos, *J. Chem. Phys.* **1992**, *96*, 1218.
[55] C. Angeli, R. Cimiraglia, S. Evangelisti, T. Leininger, J.-P. Malrieu, *J. Chem. Phys.* **2001**, *114*, 10252.
[56] C. Angeli, R. Cimiraglia, J.-P. Malrieu, *Chem. Phys. Lett.* **2001**, *350*, 297.
[57] C. Adamo, V. Barone, *J. Chem. Phys.* **1999**, *110*, 6158.
[58] Y. Zhao, D. G. Truhlar, *Theor. Chem. Acc.* **2008**, *120*, 215.
[59] T. Yanai, D. P. Tew, N. C. Handy, *Chem. Phys. Lett.* **2004**, *393*, 51.
[60] H. Iikura, T. Tsuneda, T. Yanai, K. Hirao, *J. Chem. Phys.* **2001**, *115*, 3540.
[61] C. A. Guido, D. Jacquemin, C. Adamo, B. Mennucci, *J. Phys. Chem. A* **2010**, *114*, 13402.
[62] J. P. Perdew, *Phys. Rev. B* **1986**, *33*, 8822.
[63] A. D. Becke, *J. Chem. Phys.* **1993**, *98*, 1372.
[64] A. D. Boese, J. M. L. Martin, *J. Chem. Phys.* **2004**, *121*, 3405.
[65] E. Brémond, M. Savarese, C. Adamo, D. Jacquemin, *J. Chem. Theory Comput.* **2018**, *14*, 3715.
[66] Š. Budzák, G. Scalmani, D. Jacquemin, *J. Chem. Theory Comput.* **2017**, *13*, 6237.
[67] O. Christiansen, H. Koch, P. Jørgensen, *J. Chem. Phys.* **1995**, *103*, 7429.
[68] O. Christiansen, H. Koch, P. Jørgensen, *J. Chem. Phys.* **1996**, *105*, 1451.
[69] D. Bousquet, R. Fukuda, P. Maitarad, D. Jacquemin, I. Ciofini, C. Adamo, M. Ehara, *J. Chem. Theory Comput.* **2013**, *9*, 2368.
[70] H. Nakatsuji, *Chem. Phys. Lett.* **1978**, *59*, 362.
[71] C. A. Guido, S. Knecht, J. Kongsted, B. Mennucci, *J. Chem. Theory Comput.* **2013**, *9*, 2209.
[72] O. Christiansen, H. Koch, P. Jørgensen, *Chem. Phys. Lett.* **1995**, *243*, 409.
[73] D. Tuna, Y. Lu, A. Koslowski, W. Thiel, *J. Chem. Theory Comput.* **2016**, *12*, 4400.
[74] S.-Y. Lee, S. C. Lee, *J. Chem. Phys.* **1992**, *96*, 5734.
[75] H. Bettermann, I. Dasting, W. Rauch, *J. Chem. Phys.* **1993**, *99*, 1564.
[76] A. V. Szeghalmi, V. Engel, M. Z. Zgierski, J. Popp, M. Schmitt, *J. Raman Spectrosc.* **2006**, *37*, 148.
[77] J. Guthmuller, B. Champagne, *J. Chem. Phys.* **2007**, *127*, 164507.
[78] S. Shim, C. M. Stuart, R. A. Mathies, *ChemPhysChem* **2008**, *9*, 697.
[79] A. M. Kelley, *J. Phys. Chem. A* **2008**, *112*, 11975.
[80] M. E. Casida, C. Jamorski, K. C. Casida, D. R. Salahub, *J. Chem. Phys.* **1998**, *108*, 4439.
[81] C. Hättig, *J. Chem. Phys.* **2003**, *118*, 7751.
[82] T. H. Dunning Jr., *J. Chem. Phys.* **1989**, *90*, 1007.
[83] R. A. Kendall, T. H. Dunning Jr., R. J. Harrison, *J. Chem. Phys.* **1992**, *96*, 6796.
[84] M. Feyereisen, G. Fitzgerald, A. Komornicki, *Chem. Phys. Lett.* **1993**, *208*, 359.
[85] O. Vahtras, J. Almlöf, M. W. Feyereisen, *Chem. Phys. Lett.* **1993**, *213*, 514.
[86] C. Hättig, F. Weigend, *J. Chem. Phys.* **2000**, *113*, 5154.
[87] F. Weigend, A. Köhn, C. Hättig, *J. Chem. Phys.* **2002**, *116*, 3175.
[88] A. D. Becke, *Phys. Rev. A* **1988**, *38*, 3098.
[89] J.-D. Chai, M. Head-Gordon, *Phys. Chem. Chem. Phys.* **2008**, *10*, 6615.
[90] J. P. Perdew, K. Schmidt, *AIP Conf. Proc.* **2001**, *577*, 1.
[91] S. Grimme, *J. Comput. Chem.* **2006**, *27*, 1787.
[92] J. Liu, W. Liang, *J. Chem. Phys.* **2011**, *135*, 184111.
[93] M. J. Frisch, G. W. Trucks, H. B. Schlegel, G. E. Scuseria, M. A. Robb, J. R. Cheeseman, G. Scalmani, V. Barone, G. A. Petersson, H. Nakatsuji, X. Li, M. Caricato, A. V. Marenich, J. Bloino, B. G. Janesko, R. Gomperts, B. Mennucci, H. P. Hratchian, J. V. Ortiz, A. F. Izmaylov, J. L. Sonnenberg, D. Williams-Young, F. Ding, F. Lipparini, F. Egidi, J. Goings, B. Peng, A. Petrone, T. Henderson, D. Ranasinghe, V. G. Zakrzewski, J. Gao, N. Rega, G. Zheng, W. Liang, M. Hada, M. Ehara, K. Toyota, R. Fukuda, J. Hasegawa, M. Ishida, T. Nakajima, Y. Honda, O. Kitao, H. Nakai, T. Vreven, K. Throssell, J. A. Montgomery Jr., J. E. Peralta, F. Ogliaro, M. J. Bearpark, J. J. Heyd, E. N. Brothers, K. N. Kudin, V. N. Staroverov, T. A. Keith, R. Kobayashi, J. Normand, K. Raghavachari, A. P. Rendell, J. C. Burant, S. S. Iyengar, J. Tomasi, M. Cossi, J. M. Millam, M. Klene, C. Adamo, R. Cammi, J. W. Ochterski, R. L. Martin, K. Morokuma, O. Farkas, J. B. Foresman, D. J. Fox, *Gaussian 16, Revision B.01*, Gaussian, Inc., Wallingford, CT **2016**.
[94] R. Ahlrichs, M. Bär, M. Häser, H. Horn, C. Kölmel, *Chem. Phys. Lett.* **1989**, *162*, 165.
[95] TURBOMOLE V6.3 2011, a development of University of Karlsruhe and Forschungszentrum Karlsruhe GmbH, 1989-2007, TURBOMOLE GmbH, since 2007; available at: http://www.turbomole.com, accessed January 13, 2020.
[96] O. Louant, B. Champagne, V. Liégeois, *J. Phys. Chem. A* **2018**, *122*, 972.
[97] E. Brémond, M. Savarese, N. Q. Su, A. J. Pérez-Jiménez, X. Xu, J. C. Sancho-García, C. Adamo, *J. Chem. Theory Comput.* **2016**, *12*, 459.
[98] M. Piccardo, E. Penocchio, C. Puzzarini, M. Biczysko, V. Barone, *J. Phys. Chem. A* **2015**, *119*, 2058.
[99] M. A. Rohrdanz, J. M. Herbert, *J. Chem. Phys.* **2008**, *129*, 034107.
[100] J. P. Perdew, M. Levy, *Phys. Rev. Lett.* **1983**, *51*, 1884.
[101] C.-O. Almbladh, U. von Barth, *Phys. Rev. B* **1985**, *31*, 3231.
[102] C. Hättig, *Adv. Quantum Chem.* **2005**, *50*, 37.
[103] C. Daniel, *Coord. Chem. Rev.* **2015**, *282*, 19.
[104] J. S. García, M. Boggio-Pasqua, I. Ciofini, M. Campetella, *J. Comput. Chem.* **2019**, *40*, 1420.
[105] P. Z. El-Khoury, I. Schapiro, M. Huntress, F. Melaccio, S. Gozem, L. M. Frutos, M. Olivucci, in *CRC handbook of organic photochemistry*

and photobiology, 3rd ed., Vol. 2 (Eds: A. Griesbeck, M. Oelgemöller, F. Ghetti), CRC Press, Boca Raton, FL **2012**, p. 1029.
[106] O. Falklöf, B. Durbeej, *J. Comput. Chem.* **2013**, *34*, 1363.
[107] A. Perrier, F. Maurel, D. Jacquemin, *Acc. Chem. Res.* **2012**, *45*, 1173.
[108] C. García-Iriepa, M. Marazzi, L. M. Frutos, D. Sampedro, *RSC Adv.* **2013**, *3*, 6241.
[109] P. Zhao, Y. Bu, *J. Comput. Chem.* **2018**, *39*, 1398.
[110] S. A. Mewes, F. Plasser, A. Krylov, A. Dreuw, *J. Chem. Theory Comput.* **2018**, *14*, 710.
[111] O. Falklöf, B. Durbeej, *J. Comput. Chem.* **2014**, *35*, 2184.
[112] C. Fang, B. Durbeej, *J. Phys. Chem. A* **2019**, *123*, 8485.

SUPPORTING INFORMATION

Additional supporting information may be found online in the Supporting Information section at the end of this article.

How to cite this article: Wang J, Durbeej B. How accurate are TD-DFT excited-state geometries compared to DFT ground-state geometries? *J Comput Chem*. 2020;41:1718–1729. https://doi.org/10.1002/jcc.26213